

Chapter 6

LCS and Hurricanes

In this chapter, we apply the method of using FTLE to extract Lagrangian Coherent Structures (LCS) in the manifestly turbulent wind-field data for hurricanes. A main result is the discovery of sharply defined surfaces in the flow surrounding the hurricane that govern transport of air both into and out of the storm. Furthermore, the evolution of these surfaces indicate very plainly that transport in the large-scale flow occurs via the mechanism of lobe dynamics, associated with a homoclinic tangle. The LCS method reveals that transport in hurricanes is a low-dimensional process whose salient features are adequately described by a very simple two-dimensional kinematic model that exhibits a chaotic tangle concomitant with a perturbed homoclinic connection.

We begin with an application of the LCS method to a simple kinematic model for hurricane flow. Results for the simple model will provide an insightful visual comparison with the LCS results for the actual hurricane data set. Clear similarities between the LCS in the model, and the LCS in the reanalysis data will underscore the low-dimensionality of the transport process in the hurricane flow.

6.1 Transport in a simple kinematic model

The kinematic model consists of analytic expressions for the velocity field of a single vortex in a two-dimensional uniform background flow. The velocity components of

the background flow are modeled by

$$\begin{aligned} u_b &= -\beta \\ v_b &= 0, \end{aligned}$$

with $\beta > 0$ so that the flow is from right to left.

The velocity field for a vortex with counter-clockwise flow centered at y_0 on the y -axis is given by

$$\begin{aligned} u_v &= \frac{-(y - y_0)}{x^2 + (y - y_0)^2 + \alpha} \\ v_v &= \frac{x}{x^2 + (y - y_0)^2 + \alpha}. \end{aligned}$$

Notice that the influence of the vortex decays like the inverse square of the distance from the vortex center, and that $\alpha > 0$ regularizes the velocity field at the vortex center. For the computations that follow, we take $\alpha = 0.1$.

We also consider a time-dependent forcing term of the form

$$\begin{aligned} u_f &= 0 \\ v_f &= \epsilon y \cos 2t. \end{aligned}$$

Addition of these three terms yields a very simple kinematic model for a periodically perturbed vortex in a uniform background flow:

$$\begin{aligned} u &= \frac{-(y - y_0)}{x^2 + (y - y_0)^2 + \alpha} - \beta \\ v &= \frac{x}{x^2 + (y - y_0)^2 + \alpha} + \epsilon y \cos 2t. \end{aligned} \tag{6.1}$$

Variations of system (6.1) are often provided in dynamical systems texts to illustrate a system with a homoclinic connection (as shall be verified in the next subsection). Choosing

$$\beta = \frac{1}{\sqrt{1 + 4\alpha}} \quad \text{and} \quad y_0 = \frac{1 + \sqrt{1 + 4\alpha}}{2}$$

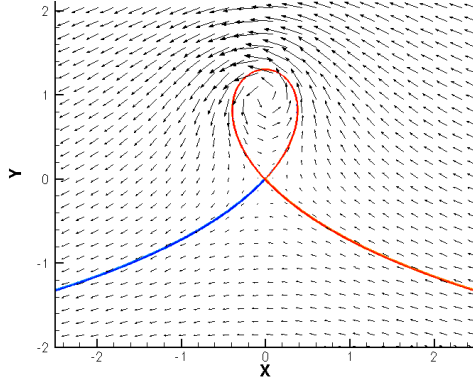


Figure 6.1: The velocity field and LCS for the unforced model. In the homoclinic loop attached to the origin, the repelling LCS (red) and the attracting LCS (blue) are exactly coincident (and hence the attracting LCS is masked by the repelling LCS). We observe here that the LCS reproduce the usual notions of stable and unstable manifolds for time-independent systems.

for a given value of α ensures that the fixed points in the unperturbed flow occur at $(0,0)$ and the point $(0,1)$ as can be easily verified.

6.1.1 Unforced case

In the unforced case ($\epsilon = 0$), the system is time-independent. The velocity field and both the repelling and attracting LCS (computed using an integration time of 10 time units) are plotted in Figure 6.1. The LCS reveal a homoclinic manifold, and coincide with the stable and unstable manifolds associated with the fixed point at the origin.

6.1.2 Forced case

We now include a relatively large forcing term by setting $\epsilon = 0.5$. The perturbation causes the intersection of the stable and unstable manifolds. As we have seen before, a single intersection induces an infinite number of intersections as the integration time is increased, and the intersections of the manifolds define lobes. Transport into and out of the region defined by the homoclinic trajectory is entirely determined by the evolution of these lobes through the action of lobe dynamics.

Figure 6.2 provides snapshots of the velocity field of the forced vortex at $t = \{0, \frac{\pi}{4}, \frac{\pi}{2}, \frac{3\pi}{4}\}$. Here we see another example where inspection of the Eulerian velocity

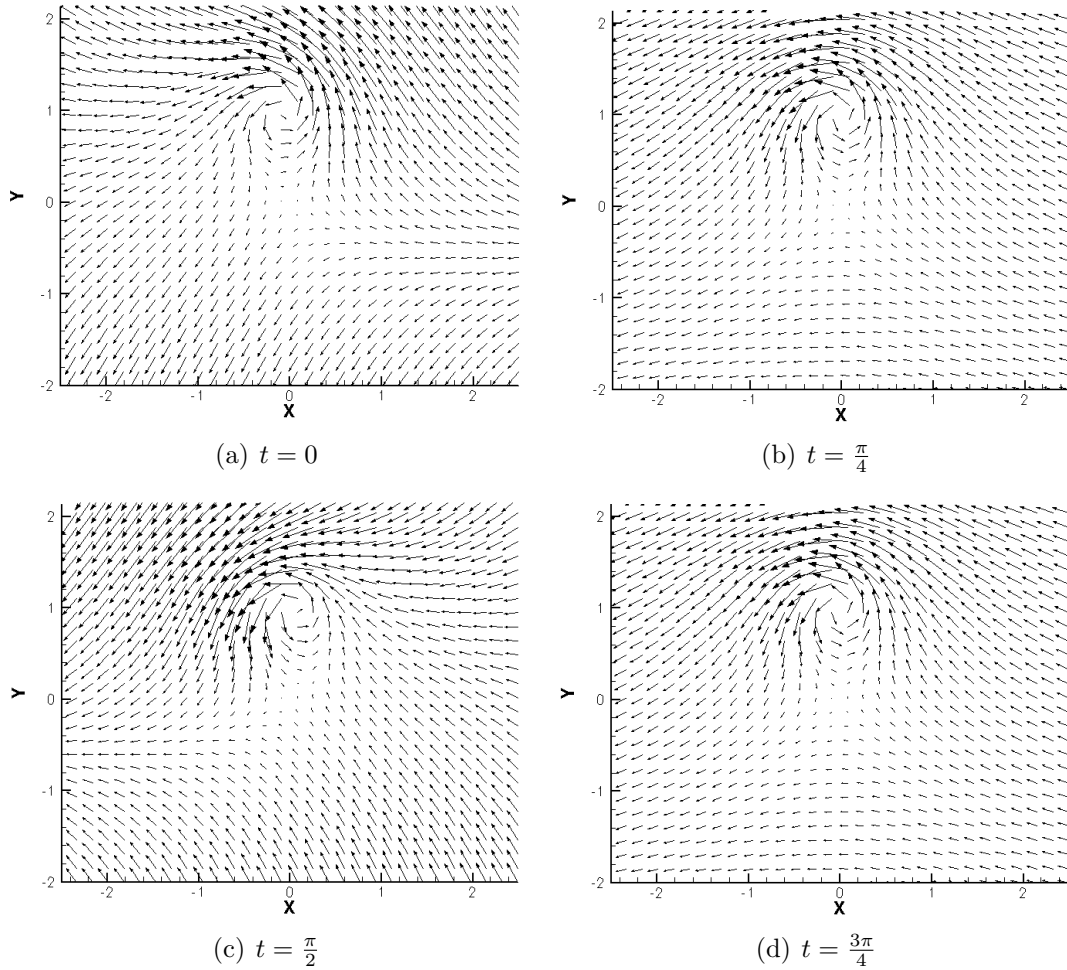


Figure 6.2: Snapshots of the velocity field in the forced model at regular intervals in time. Discerning the important transport mechanisms from snapshots of the Eulerian velocity field is not intuitive.

field alone does not elucidate the Lagrangian transport structures induced by the flow. Computation of the LCS for the forced system provides a visualization of the homoclinic tangle and consequently the transport process that occurs via lobe dynamics.

Snapshots of the LCS computed for the forced system using an integration time of 10 time units are shown in Figure 6.3. Placing passive drifters inside a lobe reveals the action of lobe dynamics. The lobe containing blue drifters is detrained out of the vortex, while the lobe containing red drifters is entrained into the vortex.

Since the forcing is periodic, the method of Poincaré maps can also be used to

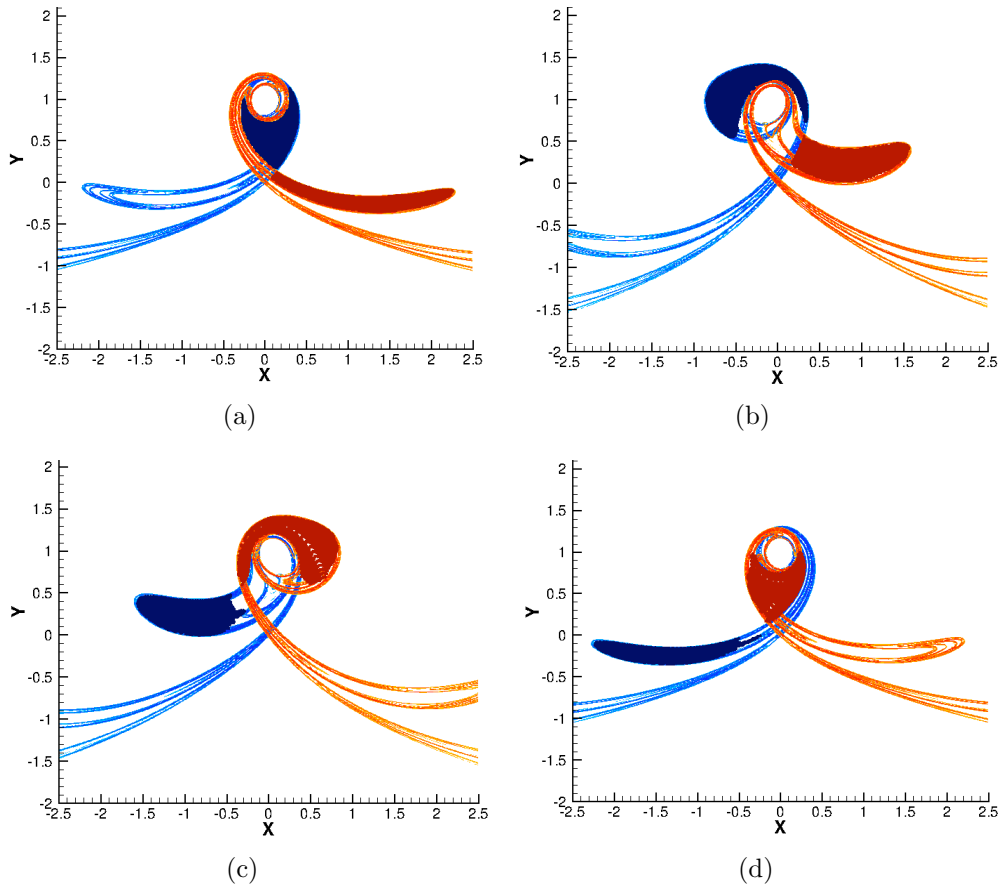


Figure 6.3: The LCS structures computed for the flow in a simple kinematic model for a periodically perturbed vortex in a linear background flow reveals a homoclinic tangle, and that transport occurs via lobe dynamics: the lobe containing red drifters is advected into the vortex, while the lobe containing blue drifters is detrained out of the vortex.

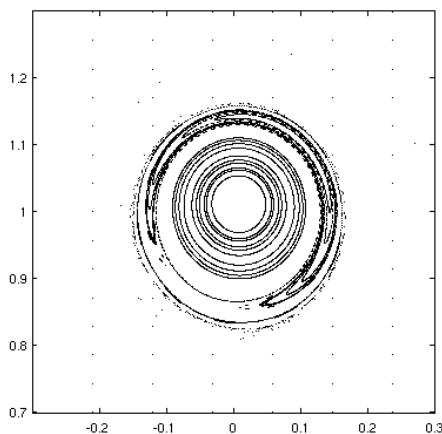


Figure 6.4: The Poincaré map computed for the simple kinematic model reveals the resonant region associated with the “eye” of the vortex as outlined by the LCS in 6.3(a). Outside the resonance region, the action of the lobes induces chaotic flow that leads trajectories to be advected out of the domain by the background flow. The map is visualized by advecting a 15×15 grid of points for 1000 periods of the forcing and plotting their locations.

analyze this flow (Figure 6.4). Analyzing the stable and unstable manifolds of the discrete map provides the intersecting manifolds and consequent lobes. Repeating this procedure over a range of starting times during the period of the perturbation reveals the evolution of the lobes. The LCS method is an entirely different approach that recovers the same result, yet has the important added feature that it can be used for systems with arbitrary time dependence (such as the raw hurricane data to be analyzed next).

The central core of the vortex in Figures 6.3(a) through 6.3(d) remains untouched by the action of the lobes and appears as a *resonance island* in the corresponding Poincaré map. Figure 6.4 shows the Poincaré map computed for this flow and depicts the resonance island that corresponds to the “eye” of the vortex in Figure 6.3(a). The LCS method indicates how the *chaotic sea* surrounding the resonance region in the Poincaré map is formed by the repeated stretching, folding, and intersection of the lobes.

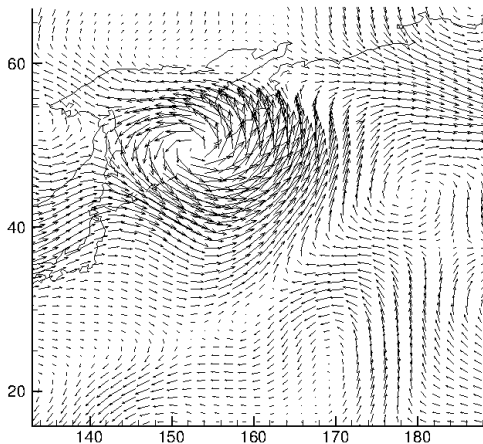


Figure 6.5: Snapshot of the velocity field above the Western Pacific at the 850mb pressure level provided by the NCAR-NCEP reanalysis data set. The prominent vortical flow indicates the flow associated with Typhoon Nabi (2005).

6.2 Transport in Typhoon Nabi

Next, we apply the method of LCS to extract coherent structures in velocity field data for a Pacific typhoon. The data is obtained from the publicly accessible NCAR-NCEP repository at <http://www.cdc.noaa.gov/cdc/data.ncep.reanalysis.html>. Specifically, we use the two-dimensional velocity field at the 850mb pressure level over the Western Pacific for late Summer of 2005. The typhoon of interest during this period is Typhoon Nabi, a category 5 tropical storm, that made landfall in Japan on September 6, 2005. A snapshot of the velocity field provided in the data set is shown in Figure 6.5.

Computation of the FTLE was performed with an integration time $T = 120$ hours. Snapshots depicting both the repelling and attracting LCS are shown in Figure 6.6. Despite the complex flow surrounding the typhoon, we readily observe that the repelling and attracting LCS accurately capture the boundary of the storm vortex, and has the shape of a homoclinic connection seen previously in the simple model. Furthermore, the evolution of the LCS reveals that the transport mechanism that governs entrainment into and detrainment out of the typhoon across this boundary is indeed lobe dynamics. For example, the region of fluid colored brown and enclosed by the intersection of the repelling and attracting LCS is a lobe that will be detrained out

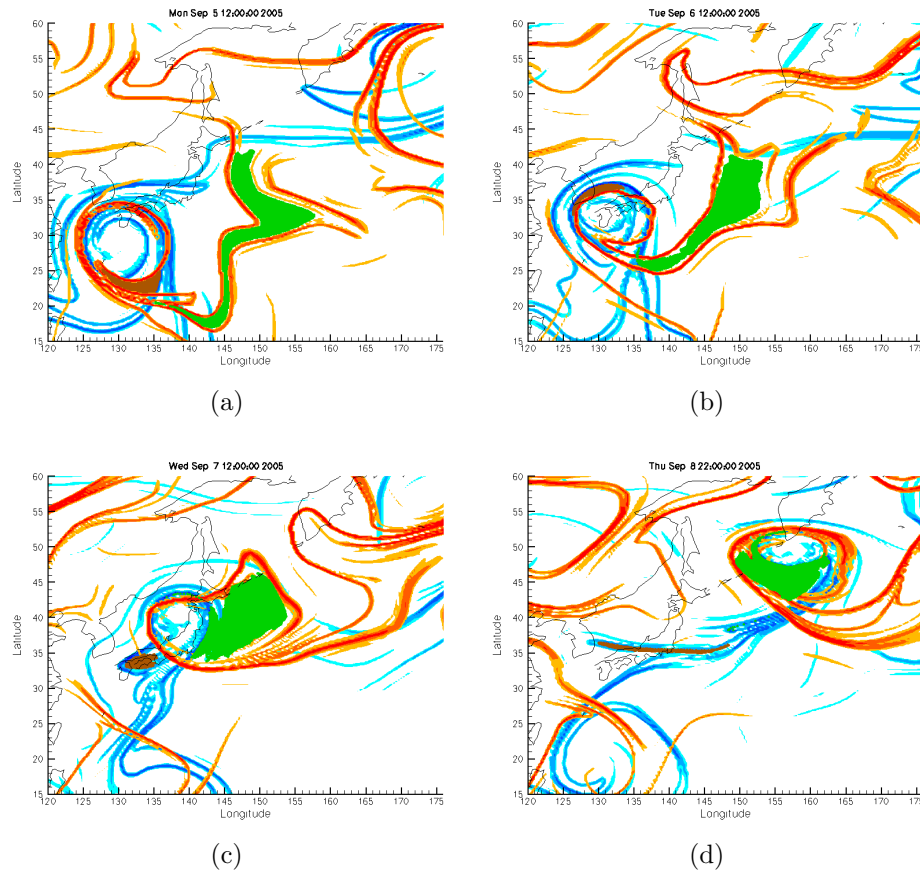


Figure 6.6: LCS for typhoon Nabi, computed from NCEP-NCAR Reanalysis Data at the 850mb pressure level. The intersections of the repelling (red) and attracting (blue) LCS define lobes that enclose regions of fluid that will be either entrained into or detrained out of the cyclone. For clarity, only two lobes have been colored although many more are evident during the animation. The LCS reveals that transport into and out of the cyclone is well-described by lobe dynamics. Indeed, the LCS forms a boundary to the cyclone that is exactly a homoclinic tangle from dynamical systems theory. Over the three day period shown, the green lobe is entrained, while the brown lobe is detrained.

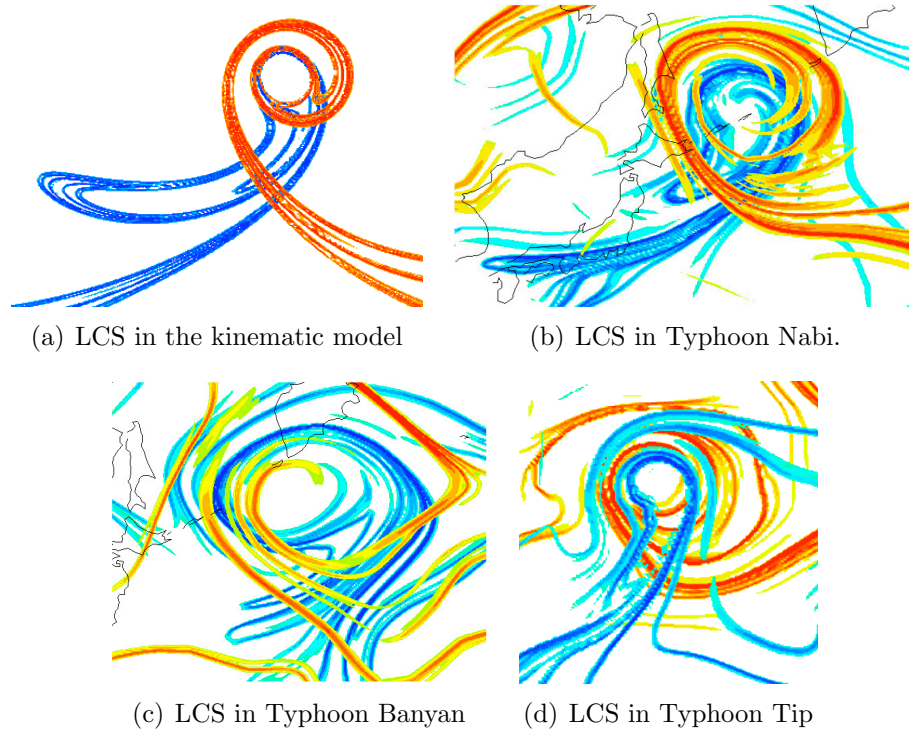


Figure 6.7: The LCS computed for the simple kinematic model is shown in (a) and compared with the LCS computed for the wind fields in three Pacific typhoons (b)-(d). The homoclinic tangle structure is evident in all three storms and indicates that lobe dynamics is a dominant transport structure in tropical storms.

of the hurricane, while the region colored green is a lobe that will be entrained into the storm. Without computing the LCS, the location of the boundary to the storm is not clear, and hence the concepts of detrainment and entrainment are ill-defined. In the literature, plots of vorticity and humidity are typically provided to indicate the size and location of a storm. These quantities are correlated with the motion of the vortex, but do not provide sharp well-defined boundaries, and consequently the transport mechanisms cannot be inferred.

Computations of the LCS for several typhoons have revealed that mixing via lobes in a homoclinic tangle is a generically dominant feature in tropical storms. Figure 6.7 shows the homoclinic tangles revealed via FTLE computations for Pacific Typhoons Tip (1979), Banyan (2005), and Nabi (2005) with the homoclinic tangle computed in the flow of the simple kinematic model provided for comparison.

The similarity between the LCS computed for Typhoon Nabi wind-field data and

the LCS computed for the simple kinematic model is quite striking. Comparing Figures 6.3(a) and 6.6(a), we see that in both cases the LCS define a boundary to the vortex, as well as lobes both inside and outside this boundary. Comparing the final figures in each sequence (Figures 6.3(d) and 6.6(d)) reveals that in both cases, the LCS dictate how the lobes will be transported by the flow, and how the processes of entrainment and detrainment from the vortex will occur. The similarity between the transport processes is most easily appreciated when the LCS are viewed as an animated movie, rather than as a sequence of individual frames. In the movies, we see that the structure of the flows is remarkably similar despite the complexity of the atmospheric flow compared with the low-dimensionality of the simple model. Computations of the LCS allow us to not only identify and characterize the dominant transport mechanism in hurricane flows, but also to observe that the essential structure of that transport mechanism can be faithfully reproduced by a simple low-dimensional model.

We remark also that careful study of the LCS computed for hurricane flows at fine detail reveals all the intricacies of the homoclinic tangle as studied theoretically in geometric mechanics. For instance, the action of the Smale horseshoe map and the first iteration in the formation of a Cantor set can be plainly discerned in the evolution of the LCS. As in our discussion in Chapter 2, these concepts are typically studied with regard to the Poincaré maps of periodically perturbed systems and are presented in abstraction, whereas here we see that the FTLE method for extracting LCS uncovers these very same notions in the seemingly unrelated turbulent and aperiodic flows of actual hurricane data, and presents them in a way that their evolution can be observed naturally through animation. Figure 6.8 illustrates how the central “third” region (shaded brown) is advected out of the storm, while the outer two “thirds” (shaded green) remain inside the storm, just as is prescribed by a single iteration of the Smale horseshoe map in the formation of the Cantor set.

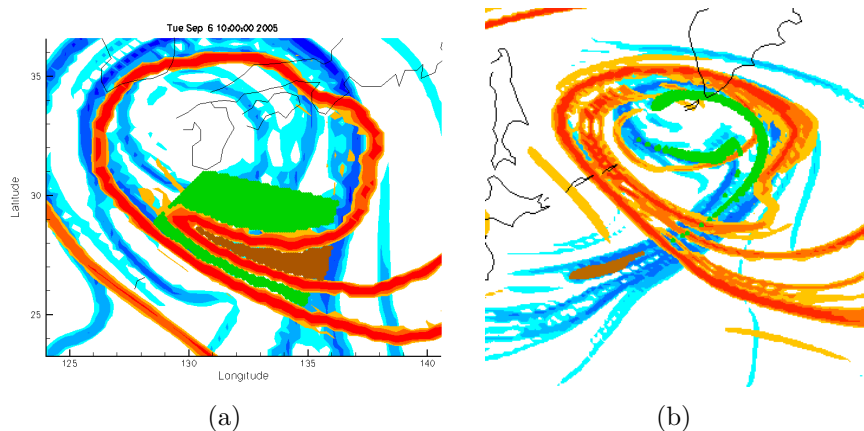


Figure 6.8: The action of lobe dynamics in the homoclinic tangle induces a map that, as has been shown by Smale, leads to the formation of a Cantor set when iterated. Here we see the first iteration of the horseshoe map in the flow of the typhoon: the middle ‘third’, colored brown, is removed from the storm, while the two green outer ‘thirds’ remain.

6.3 Eye-wall structures in Hurricane Isabel

The study of flow in Typhoon Nabi was concerned with synoptic-scale flow. We now consider three-dimensional flow in the vicinity of a hurricane eye-wall. Recent observational data obtained during hurricanes Katrina (2005) and Rita (2005) indicate that storm intensity is intricately related to fine-scale processes such as *eyewall replacement* — a process in which the eyewall of a storm disintegrates and is replaced by an eyewall of larger radius and lower wind speed, resulting in decreased intensity [Houze 2007]. As was the case with Hurricane Rita, the new eyewall can subsequently contract, causing rapid storm intensification. This process of rapid intensity fluctuation has also been observed in high-resolution model data [Chen 2007, Houze 2007]. These observations emphasize that an understanding of the detailed dynamics of the hurricane eyewall is crucial to accurate predictions of storm intensity. Furthermore, the stability of a hurricane, and whether it will tend to decay or intensify, is dependent to some degree on the moisture and energy content of the air parcels it entrains from the large-scale flow. Hence, an understanding of the transport structures and mechanisms within the hurricane is a prerequisite for accurate intensity prediction. A lack of understanding with regard to the structural dynamics and transport processes

in hurricanes could well be part of the explanation for the current inability among the forecasting community to decrease intensity prediction errors despite exponentially increasing computing power¹.

In a three-dimensional flow model for Hurricane Isabel (2003) computed using the WRF model [Kuo 2003], LCS proves to be an effective method for analyzing transport structures near the eyewall. Figure 6.9 shows the extracted eyewall as visualized using LCS. Meteorologists typically define the eyewall as the locations of maximum wind speed on rays emanating from the eye of the storm. This definition, although simple to visualize, is an intrinsically Eulerian approach that, as has been shown in many applications, fails to capture the Lagrangian quantities necessary to understand transport in time-dependent flows [Shadden 2007]. Recently, attempts have been made to determine the instantaneous vortex filament about which the hurricane is rotating; however, this approach yields only the center of the vortex and no information about transport in the flow [Weinkauff 2007]. LCS, on the other hand, necessarily encodes information about the Lagrangian transport of tracers within the flow and is a rigorous barrier to transport. Thus, the surface revealed by the LCS is a precise definition of the eyewall that is consistent with the Lagrangian dynamics of the flow.

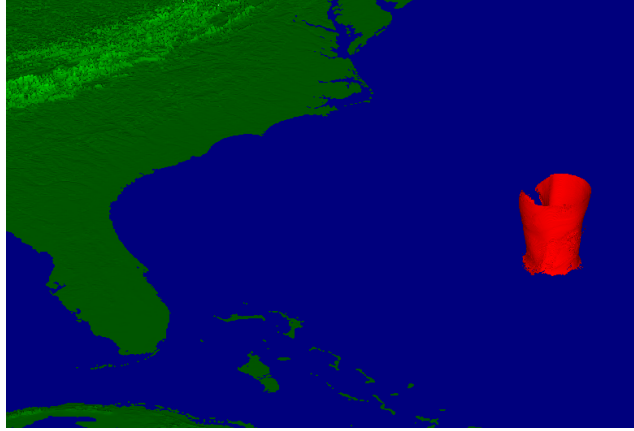
The insights into transport near the hurricane eyewall provided by the LCS are readily discerned by observing the trajectories of passive drifters placed in the various regions delineated by the LCS. For example, Figure 6.10 indicates drifters with initial positions located inside the eyewall (red) and outside the eyewall (blue). When these drifters are advected by the flow, as depicted in Figure 6.11, the red drifters remain inside the eye of the storm while the blue drifters are ejected from the storm into the upper atmosphere.

The green drifters are initially located in a lobe region protruding from the southwestern edge of the eye. This lobe region represents air mass that will be detrained from the eye region and eventually ejected into the upper atmosphere, as evidenced by the trajectories of the green drifters. Already, we begin to see that the LCS

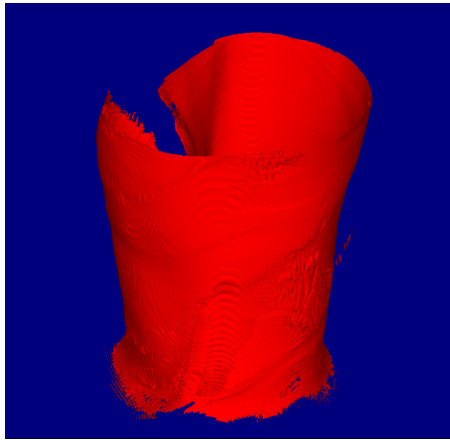
¹See the forecast error analysis at <http://www.nhc.noaa.gov/verification/verify5.shtml>

summarizes and describes the transport processes near the eyewall.

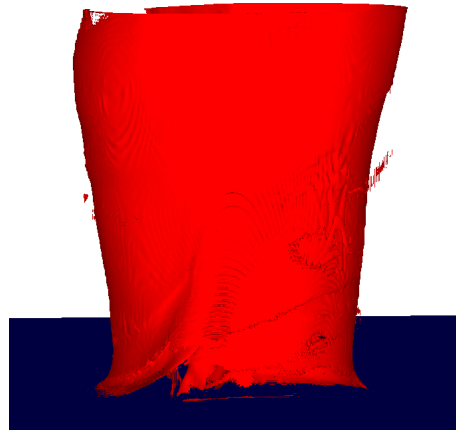
It is hoped that the insights gained from further explorations in both the large-scale and the near-eyewall flow will directly inform the development of improved hurricane modeling and forecasting, as well as the types and locations of *in situ* data measurements (using dropsondes, for example) that will allow for optimal data collection, and the most accurate prediction of storm evolution.



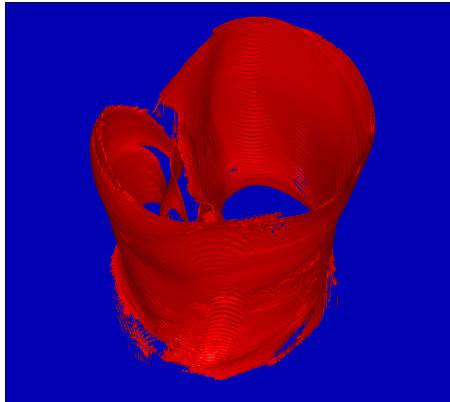
(a) The eyewall of Hurricane Isabel as visualized using the repelling LCS. The eyewall reaches an approximate height of 8km above sea-level.



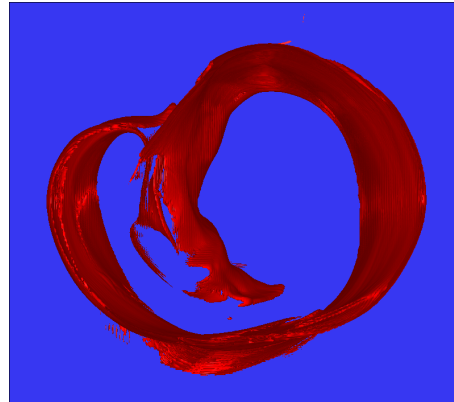
(b) Side view.



(c) View from the ocean surface.



(d) Oblique view from above.



(e) Top view indicating a lobe structure protruding from the southwest corner of the main eye region.

Figure 6.9: The repelling LCS reveals the precise location and structure of the eyewall for Hurricane Isabel (2003). Figure 6.9(a) shows the eyewall in the Atlantic during the approach of Hurricane Isabel to the mainland, while figures 6.9(b)-6.9(e) show the three-dimensional structure of the eyewall from various viewpoints.

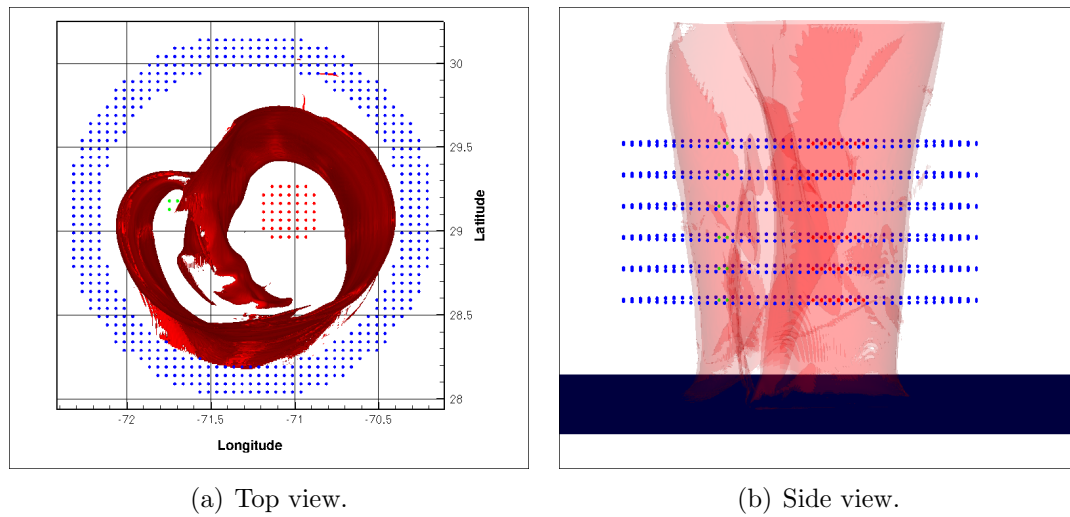


Figure 6.10: The eyewall, as revealed by the LCS, is a coherent structure that governs transport near the eye of the hurricane. This property is revealed by placing passive drifters in the different regions defined by the LCS and observing their trajectories under the action of the flow. The initial placement of the drifters is shown here: red drifters are placed well inside the eyewall, green drifters are placed in a lobe structure that will be detrained from the eye, and an annulus of blue drifters is placed outside the eyewall.

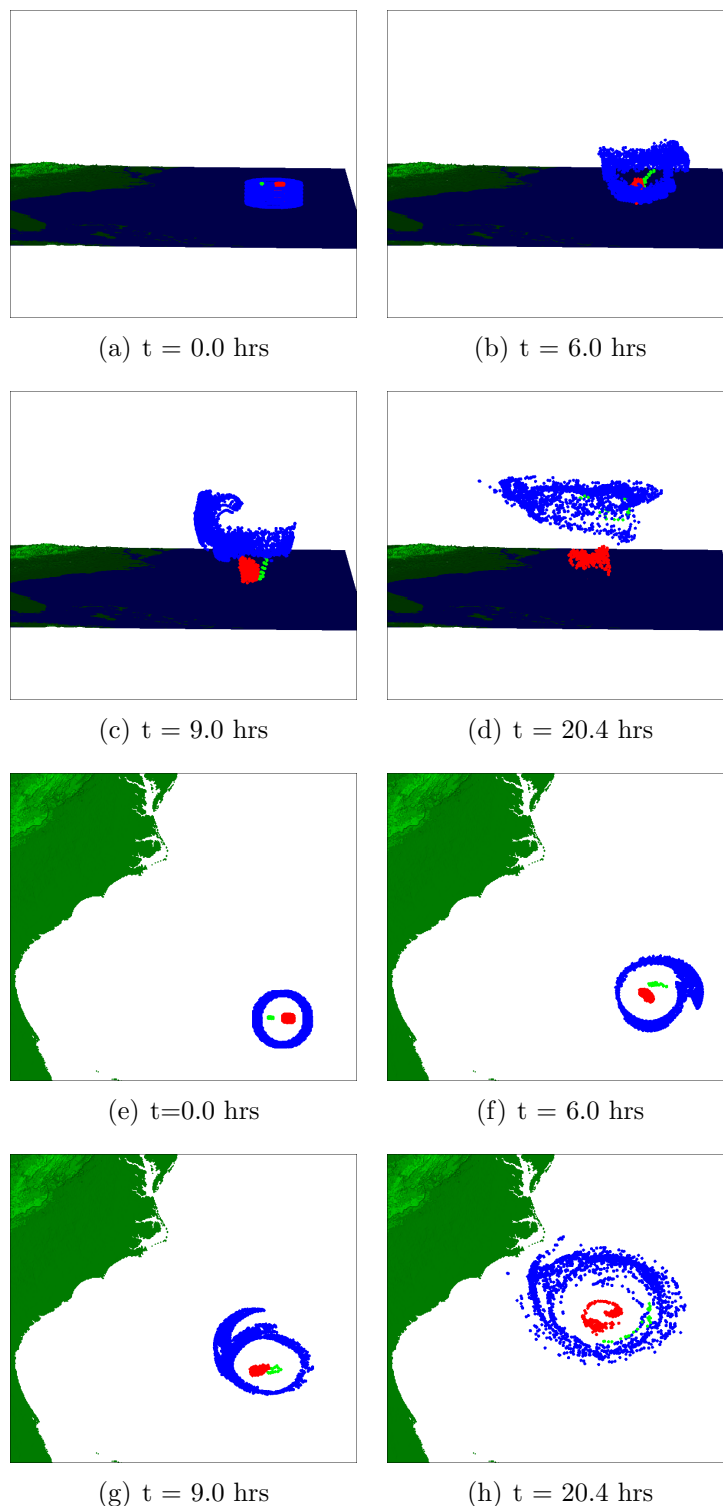


Figure 6.11: The drifters initially placed as depicted in Figure 6.10 (notice that they are strategically placed relative to the LCS) are advected forward in the flow. Snapshots of the drifter trajectories are shown here from above and from the side. Red particles within the eyewall remain near the ocean surface, while the blue particles are ejected into the upper atmosphere. The green particles are eventually detrained from the eye, and follow the blue drifters into the upper atmosphere.